

CCD SPECKLE OBSERVATIONS OF BINARY STARS FROM THE SOUTHERN HEMISPHERE. II. MEASURES FROM THE LOWELL-TOLOLO TELESCOPE DURING 1999

ELLIOTT HORCH¹

Chester F. Carlson Center for Imaging Science, Rochester Institute of Technology, 54 Lomb Memorial Drive, Rochester, NY 14623-5604; horch@cis.rit.edu

OTTO G. FRANZ¹

Lowell Observatory, 1400 West Mars Hill Road, Flagstaff, AZ 86001; ogf@lowell.edu

AND

ZORAN NINKOV

Chester F. Carlson Center for Imaging Science, Rochester Institute of Technology, 54 Lomb Memorial Drive, Rochester, NY 14623-5604; ninkov@cis.rit.edu

Received 2000 June 20; accepted 2000 July 20

ABSTRACT

Speckle observations of 145 double stars and suspected double stars are presented and discussed. On the basis of multiple observations, a total of 280 position angle and separation measures are determined, as well as 23 high-quality nondetections. All observations were taken with the (unintensified) Rochester Institute of Technology fast-readout CCD camera mounted on the Lowell-Tololo 61 cm telescope at the Cerro Tololo Inter-American Observatory during 1999 October. We find that the measures, when judged as a whole against ephemeris positions of binaries with very well-known orbits, have root mean square deviations of $1^{\circ}8 \pm 0^{\circ}3$ in position angle and 13 ± 2 mas in separation. Eleven double stars discovered by *Hipparcos* were also successfully observed, and the change in position angle and/or separation since the *Hipparcos* observations was substantial in three cases.

Key words: astrometry — binaries: close — binaries: visual — techniques: interferometric

1. INTRODUCTION

In the first paper of this series, the use of a large-format, fast-readout CCD system for the determination of high-quality relative astrometry of binary stars via the technique of speckle interferometry was demonstrated (Horch, Ninkov, & Slawson 1997, hereafter Paper I). The data presented were obtained at the University of Toronto 60 cm telescope, which at the time was located at Las Campanas, Chile. It was noted in that work that, although the Southern Hemisphere has a long tradition of visual and interferometric binary star observations by skilled observers such as van den Bos, Rossiter, Finsen, and others, at the present time there are few data emerging from the south. In the speckle era, several investigators such as Morgan et al. (1978), Morgan, Beckmann, & Scaddan (1980); Morgan et al. (1982), Argue et al. (1984), White et al. (1991), and Horch et al. (1996) have contributed measures, but the most sustained effort that continued the work of the visual observers to obtain high-quality orbits of southern double stars was the program of the Center for High Angular Resolution Astronomy (CHARA) group when they were observing regularly at the Cerro Tololo Inter-American Observatory (CTIO) 4 m telescope between 1989 and 1996 (McAlister, Hartkopf, & Franz 1990; Hartkopf et al. 1993; Hartkopf et al. 1996). Unfortunately, these measures do not span a long enough time period to permit definitive orbit revisions of the classic sample of southern visual binaries.

In this paper, we present results from a total of 303 speckle observations obtained during October of 1999 using essentially the same camera system and observing technique as in Paper I, but with the Lowell-Tololo 61 cm

telescope at CTIO. Since the work presented here falls short of a sustained southern observing program, our approach has been to attempt to maximize the impact for future orbit redeterminations by focusing mainly on objects with visual orbits in the catalog of Worley & Heintz (1983). Many of these orbits are of marginal or poor quality by current standards and are prime examples of how speckle interferometry can be used to provide necessary data to make significant progress in the orbital solutions in the coming years. This is especially important with the advent of *Hipparcos* parallaxes for these objects (ESA 1997) and the promise of continued improvements in the distance measures from the *Full-Sky Astrometric Mapping Explorer (FAME)* and the *Space Interferometry Mission (SIM)* within the next decade. In addition to these well-known southern visual binaries and calibration objects, we also observed some stars discovered to be double or suspected of duplicity by *Hipparcos* to determine any change in the relative position since the *Hipparcos* observation in the former case and to attempt to confirm duplicity in the latter.

2. OBSERVATIONS

All observations presented here were obtained during the two-week period from 1999 October 5 to 1999 October 18 (UT). As in Paper I, the CCD used was a Kodak KAF-4200 chip set inside a Photometrics, Ltd., camera head available as part of the solid state sensor development program at Rochester Institute of Technology (RIT). This device has 9 μm square pixels and is front illuminated, providing a quantum efficiency of 30%–40% through the visible range. The electronics module used to read out the chip was somewhat faster than the earlier version discussed in Paper I and operated at a rate of 500 kpixel s^{-1} . This allowed for a 1024-frame sequence of speckle data to be obtained in approximately 1 to 2 minutes, depending on the pixel-

¹ Visiting Astronomer, Cerro Tololo Inter-American Observatory, National Optical Astronomy Observatories.

TABLE 1
SCALE AND ORIENTATION RESULTS FOR 1999 OCTOBER

Focal Ratio	CCD Binning	Type of Measure	Zero-Point Angle (deg)	Scale (mas pixel ⁻¹)
f/75	4 × 4	Aperture mask	0.47 ± 1.23	163.6 ± 0.6
		Star trails	0.34 ± 0.13	...
		Trapezium	-0.02 ± 0.05	162.9 ± 0.4
Final adopted value:			0.35 ± 0.17	163.6 ± 0.6
f/13.5	1 × 1	Aperture mask	...	227.3 ± 1.3
		Star trails	-0.06 ± 0.02	...
		Final adopted value:	-0.06 ± 0.02	227.3 ± 1.3

binning factor used. Two filters were used: Bessel V ($\lambda_0 = 541$ nm, $\Delta\lambda_{\text{FWHM}} = 88$ nm) and R ($\lambda_0 = 644$ nm, $\Delta\lambda_{\text{FWHM}} = 128$ nm; Bessel 1990).

The Lowell-Tololo Telescope has two available secondary mirrors; one provides a beam of f/13.5 and the other f/75. The f/75 secondary was convenient for providing the magnification normally desired for speckle observations and was used for about 90% of the data taken. In this configuration, the CCD pixels were typically binned 4 × 4 to achieve a pixel scale that approximated critical sampling (however, a handful of observations were binned 3 × 3); in actual fact, the diffraction-limited point-spread function of the telescope was marginally undersampled. As discussed in Paper I, our analysis technique includes the subpixel sensitivity map of Kavalajiev & Ninkov (1998) for the KAF-4200 chip to derive the most accurate astrometry from undersampled data. At f/75, the pixel scale and detector orientation (relative to the equatorial celestial coordinate system) were measured with the use of a two-hole mask placed over the telescope aperture. The pixel scale was then obtained as in Paper I, except that instead of using stellar spectra from Gunn & Stryker (1983) in the determination of the effective center wavelength of the mask observations (which is dependent on the spectral type of the star observed because of the wide passband), the spectra from Jacoby, Hunter, & Christian (1984) were used. The mask was oriented by pointing the telescope to the horizontal while it was on the meridian and using a plumb bob to position the center line between the holes. The fringes obtained when

observing a bright unresolved star were then aligned east-west by definition. The technique of trailing stars across the detector with the tracking off was also used to provide an independent measure of the detector's zero-point angle. The results of these two types of measures were checked against a series of short exposures of the Trapezium (θ^1 Orionis), where the scale and zero-point angle were determined with the aid of astrometry in the literature (van Altena et al. 1988). All scale and orientation values obtained are shown in Table 1. For the determination of position angles and separations listed in the next section, we used the mask scale value and a weighted average of the angle values determined with the mask and the star trails, as shown.

The f/13.5 secondary was used for observations on two nights. In this configuration, the diffraction-limited point-spread function of the telescope was substantially undersampled, and the analysis of these data relied heavily on the undersampling correction method outlined in Paper I. It may be that measures obtained with f/13.5 are of lower quality than those obtained with the f/75 arrangement, but there are too few observations to make a definitive statement at present. Scale and detector orientation measures for f/13.5 are also shown in Table 1. The location of the secondary mirror inside the f/13.5 housing made it impossible to use the plumb bob method to orient the mask, so we have adopted the star trail value for the zero-point angle here. No Trapezium images were taken at f/13.5.

Our basic reduction scheme continues to be the weighted least-squares fit to the average power spectrum of the speckle frames making up an observation, and it is fully described in Paper I. This technique necessitates an observation of an unresolved source (a single star) close in time and in sky position to the double star of interest, which we chose from the Bright Star Catalogue (Hoffleit & Jaschek 1982). For the observations discussed here, we attempted to find a single suitable point source for two to four binaries that were all close together on the sky to make the observing more efficient. In the course of reducing these data, the seeing is estimated for each object, and two basic criteria are used to determine if a measure is of high quality: (1) the final reduced χ^2 of the power spectrum fit and (2) the number of pixels used in the fit (which is determined by power spectrum signal-to-noise estimates and other factors). The position angle ambiguity inherent in the power spectrum approach was resolved by creating a low-quality reconstructed image from two subplanes of the image bispectrum.

Seeing conditions during the run ranged typically between 1".6 to 2".3, much worse than the observations presented in Paper I but consistent with seeing measures obtained by the CTIO 4 m telescope during the same nights. Since seeing is known to affect speckle measurement

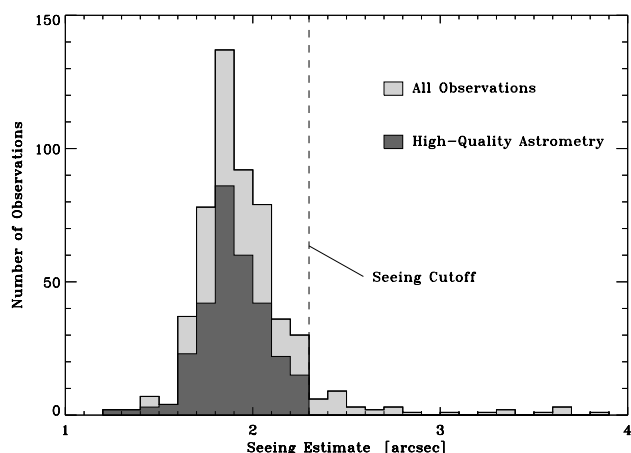


FIG. 1.—Seeing histogram for the observations obtained. The lighter histogram is for all observations during the run (except a few judged at the outset to be too poor to attempt analysis), and the darker histogram is for only those objects for which the full reduction process succeeded. This is the same sample of objects that appears in Table 2.

precision (see e.g., Horch et al. 1997), it was decided that all observations with seeing estimates of greater than $2''.3$ would be removed from further consideration. This affects relatively few stars, but gives greater assurance that the astrometry determined from the remaining stars is of high quality. Seeing histograms for both the full sample of observations and the subset of observations judged to be of high quality are shown in Figure 1.

3. RESULTS

3.1. Measures

Table 2 contains the main body of astrometric results from the data set. The columns give (1) the Aitken Double Star (ADS) Catalog number or, if none, the Bright Star Catalog (HR) number or, if none, the Durchmusterung (BD, CP, or CD) number; (2) the discoverer designation; (3) the HD number; (4) the *Hipparcos* Catalogue number; (5) the right ascension and declination in J2000.0 coordinates, which is the same as the identification number in the Washington Double Star (WDS) Catalog (Worley & Douglass 1997) for all objects that have WDS entries; (6) the observation date in fraction of the Besselian year; (7) the observed position angle (θ), in degrees, with north through east defining the positive sense of θ ; (8) the observed separation (ρ) in arcseconds; (9) the center wavelength of the filter used to make the observation, in nanometers; and (10) the FWHM passband, also in nanometers. The position angles have not been corrected for precession and are appropriate for the epoch of observation shown. Position angles and separations are shown without uncertainty estimates, but a reasonable uncertainty estimate for any measure shown may be obtained by combining the measurement precision given in the next subsection with the uncertainty in the scale and detector orientation given in Table 1 in quadrature using standard error formulas.

Eleven of the objects in Table 2 were discovered by *Hipparcos* and have no other orbital data at present. Table 3 gives further information concerning these objects, including the change in position angle and separation since the *Hipparcos* observations. The column headings are as

follows: (1) *Hipparcos* Double Star number; (2) *Hipparcos* Catalogue number; (3) the total Johnson V magnitude of the system; (4) the magnitude difference of the system as it appears in the *Hipparcos* Catalogue; (5) the parallax determined by *Hipparcos*, in mas; (6) the position angle and (7) separation of the components as determined by *Hipparcos*, in degrees and arcseconds, respectively; and (8) and (9) the difference between the values in columns (5) and (6) and the measures appearing in Table 2. Three objects of the 11 appear to be relatively fast moving, namely, HDS 107, HDS 2957, and HDS 3152. The latter two are observable from northern sites and all three warrant continued attention in the coming years.

3.2. Detection and Measurement Capability

In order to characterize the accuracy and precision of our measures, we selected the subset of objects from Table 2 that have had recent orbit revisions that include substantial speckle data drawn from Hartkopf, McAlister, & Franz (1989), Hartkopf, Mason, & McAlister (1996), and other sources (Mason 1997; W. I. Hartkopf 1998, private communication; Mason, Douglass, & Hartkopf 1999). Table 4 contains the average deviation and root mean square (rms) deviation from the ephemeris positions for our measures of these objects, subject to orbit quality criteria. The orbits used have been published with uncertainties in the orbital parameters, and therefore the uncertainty in the ephemeris positions can be calculated. To ensure that the portion of the residual due to the uncertainty of the orbit was kept to a minimum (thereby allowing us to study the astrometric precision of the measures obtained), only orbits with the smallest uncertainties in ephemeris positions were used in deriving the results in Table 4. For studying the position angle determinations, orbits with ephemeris uncertainties of less than 1° were used, while for the separation only orbits with separation uncertainties of less than 6.5 mas were considered.

Figures 2a and 2b show residual plots for separation and position angle, based on ephemeris positions derived from the orbit. Open circles denote orbits whose uncertainty in the ephemeris position was above the criterion listed in

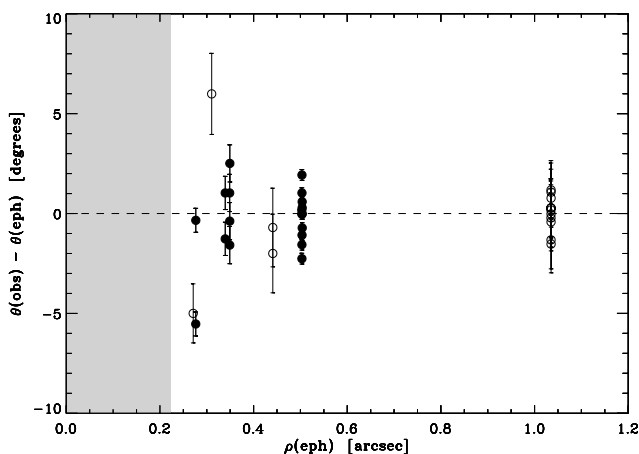


Fig.2a

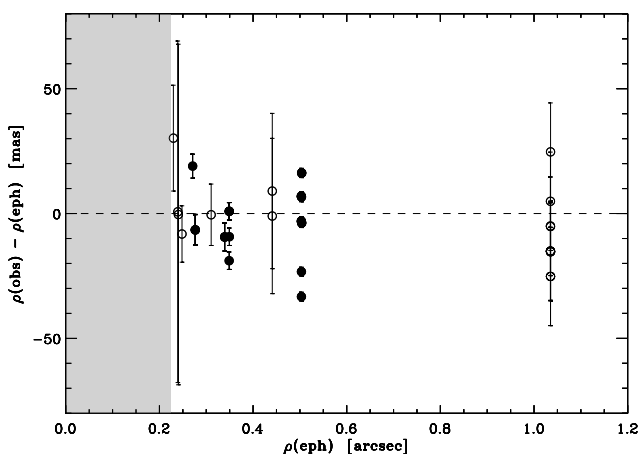


Fig.2b

FIG. 2.—(a) Position angle residuals plotted as a function of ephemeris separation for all objects in Table 2 having orbits determined with speckle data. (b) Separation residuals plotted as a function of ephemeris separation for the same set of observations. In both plots, filled circles are data points from the highest quality orbits that were used to derive the values in Table 4, open circles are speckle orbits of lower quality (not used in Table 4), and the error bars are the ephemeris uncertainties as calculated from the published orbital parameters. The gray band marks the region below the diffraction limit of the telescope (at V).

TABLE 2
DOUBLE STAR SPECKLE MEASURES

HR, ADS, DM, etc. (1)	Discoverer Designation (2)	HD (3)	HIP (4)	WDS (α, δ J2000.0) (5)	Date (1900+) (6)	θ (deg) (7)	ρ (arcsec) (8)	λ (nm) (9)	$\Delta\lambda$ (nm) (10)
HR 23	HDO 181	469	730	00090—5400	99.7676	61.4	0.29	541	88 ^a
	99.7731	63.0	0.27	541	88 ^a
ADS 111	BU 391AB	493	761	00094—2759	99.7813	260.3	1.42	541	88
	99.7950	260.1	1.44	644	128
HR 127	I 260CD	2884	2484	00316—6258	99.7676	276.9	0.58	541	88
	99.7731	276.6	0.58	541	88
	99.7786	276.4	0.59	541	88
	99.7839	276.9	0.58	644	128
ADS 449	MCA 1Aa	2913	2548	00324+0657	99.7867	278.1	0.29	541	88
ADS 490	HO 212AB	3196	2762	00352—0336	99.7813	295.8	0.24	541	88
	99.7950	308.0	0.24	541	88
ADS 520	BU 395	3443	2941	00373—2446	99.7650	287.7	0.51	541	88 ^a
	99.7650	288.4	0.50	644	128
	99.7676	286.8	0.50	541	88
	99.7758	287.5	0.50	541	88 ^c
	99.7840	288.1	0.50	644	128
	99.7950	287.7	0.51	644	128 ^b
BD—04 85	HDS 95	4061	3385	00430—0351	99.7813	337.9	0.90	541	88
CP—63 72	COO 3	4294	3489	00445—6230	99.7813	65.9	2.34	541	88
	99.7841	66.2	2.32	644	128
BD—17 132	MLF 1	4338	3576	00457—1625	99.7868	199.2	2.89	541	88
CP—61 37	HDS 107	4774	3804	00489—6022	99.7840	301.7	0.85	644	128
HR 257	5276	4200	00536—6252	99.7841	...	<0.26	644	128
CP—67 62	I 48	5756	4512	00579—6634	99.7842	9.6	0.33	644	128 ^a
HR 322	SLR 1AB	6595	5165	01061—4643	99.7677	259.9	0.29	541	88 ^a
	99.7731	78.8	0.29	541	88 ^b
	99.7840	77.8	0.28	644	128 ^b
HR 331	RST 3352	6767	5300	01078—4129	99.7650	148.9	0.29	541	88 ^c
	99.7650	146.9	0.29	644	128 ^c
	99.7732	331.3	0.26	541	88 ^a
	99.7732	332.2	0.25	541	88 ^a
	99.7841	328.5	0.29	644	128
CP—55 241	RST 1205AB	6882	5348	01084—5515	99.7759	94.8	0.53	541	88
	99.7786	95.6	0.56	541	88
	99.7842	94.8	0.55	644	128
CP—66 87	HDS 154	7174	5514	01106—6555	99.7950	289.3	0.67	644	128
HR 377	HJ 3423AB	7788	5896	01158—6853	99.7868	321.8	4.96	541	88
	99.7950	321.9	4.99	644	128
CP—67 81	HJ 3426	7916	5992	01171—6624	99.7814	330.2	2.43	541	88
ADS 1081	STF 113A-BC	8036	6226	01198—0031	99.7704	16.3	1.60	541	88
	99.7704	16.6	1.60	644	128
	99.7786	16.2	1.60	541	88
	99.7840	16.6	1.58	644	128
	99.7868	16.4	1.61	541	88
CP—70 64	I 263	8519	6377	01220—6943	99.7950	263.8	0.53	644	128
ADS 1123	BU 1163	8556	6564	01243—0655	99.7651	34.1	0.34	644	128 ^b
	99.7759	31.2	0.35	541	88 ^b
	99.7759	210.0	0.35	644	128 ^a
	99.7840	212.6	0.33	644	128 ^a
CD—48 367	RST 33	8821	6693	01259—4754	99.7841	302.0	1.11	644	128
CD—30 540	HJ 3447	9906	7463	01361—2954	99.7677	167.1	0.78	541	88
	99.7704	167.5	0.78	541	88
	99.7704	167.2	0.78	644	128
	99.7732	167.7	0.79	541	88
	99.7814	167.1	0.78	541	88
	99.7841	167.2	0.78	644	128
	99.7841	167.4	0.79	644	128
	99.7950	169.1	0.81	541	88
HR 466	KUI 7	10009	7580	01376—0924	99.7732	329.1	0.27	541	88 ^c
	99.7814	323.9	0.27	541	88 ^c
ADS 1339	STF 147	10453	7916	01417—1119	99.7814	94.7	0.68	541	88
ADS 1345	A 1	10508	7968	01424—0645	99.7732	66.1	0.81	644	128
	99.7814	244.6	0.86	541	88 ^b
	99.7841	71.7	0.85	644	128 ^a

TABLE 2—Continued

HR, ADS, DM, etc. (1)	Discoverer Designation (2)	HD (3)	HIP (4)	WDS (α, δ J2000.0) (5)	Date (1900+) (6)	θ (deg) (7)	ρ (arcsec) (8)	λ (nm) (9)	$\Delta\lambda$ (nm) (10)
CD—25 704	HJ 3461AB	10830	8209	01456—2503	99.7950	65.5	0.86	541	88 ^a
HR 519	10934	8240	01461—5049	99.7760	...	<0.22	541	88
ADS 1538	STF 186	11803	8998	01559+0151	99.7677	241.8	1.04	541	88 ^c
ADS 1615	STF 202AB	12446—7	9487	02020+0246	99.7678	273.0	1.83	541	88
BD—18 394	HTG 1	14001	10542	02158—1814	99.7678	141.8	1.76	541	88
CD—30 852	BU 738	14882	11131	02232—2952	99.7815	212.6	1.58	541	88
CD—25 979	HDS 325	15634	11644	02302—2511	99.7652	74.4	0.58	541	88
HR 804	STF 299	16970	12706	02433+0314	99.7734	298.0	2.48	541	88
CP—67 181	FIN 333	17326	12717	02434—6643	99.7842	...	<0.26	644	128
BD +18 347	STF 305AB	17332	13027	02475+1922	99.7733	309.1	3.67	541	88
HR 832	17491	13064	02479—1228	99.7870	...	<0.26	644	128
ADS 2242	BU 741AB	18455	13772	02572—2458	99.7652	337.8	1.01	541	88
HR 911	18884	14135	03023+0405	99.7787	...	<0.22	541	88
HR 968	HJ 3556AB-C	20121	14913	03124—4425	99.7816	191.5	3.89	541	88
HR 968	JC 8AB	20121	14913	03124—4425	99.7816	171.5	0.78	541	88
ADS 2463	SEE 23	20610	15382	03184—2231	99.7680	270.3	0.34	541	88
BD—01 469	AC 2AB	20559	15383	03184—0056	99.7679	254.8	1.23	541	88
CP—59 298	HDS 505	25614	18731	04007—5840	99.7653	266.1	0.30	541	88 ^a
HR 1264	25705	18744	04009—6210	99.7653	...	<0.22	541	88
CD—42 1400	HDS 530	26612	19515	04108—4200	99.7817	...	<0.22	541	88
ADS 3072	BU 547AB	26722	19740	04139+0916	99.7736	341.7	1.24	541	88
HR 1357	GLE 1	27463	19917	04163—6057	99.7735	343.2	0.29	541	88 ^b
ADS 3135	STT 79	27383	20215	04199+1631	99.7817	311.6	0.34	541	88 ^a
ADS 3159	BU 744AB	27710	20347	04215—2544	99.7654	21.6	0.27	541	88 ^a
ADS 3169	STT 82AB	27691	20440	04227+1503	99.7680	343.8	1.33	541	88
ADS 3174	STF 535	27762	20472	04233+1123	99.7680	281.8	1.19	541	88
ADS 3206	KUI 17AB	27962	20648	04255+1756	99.7762	340.3	1.85	541	88
ADS 3230	BU 311	28312	20765	04269—2405	99.7655	318.5	0.48	541	88 ^b
ADS 3264	STF 554AB	28485	20995	04301+1538	99.7681	18.0	1.64	541	88

TABLE 2—Continued

HR, ADS, DM, etc. (1)	Discoverer Designation (2)	HD (3)	HIP (4)	WDS (α, δ J2000.0) (5)	Date (1900+) (6)	θ (deg) (7)	ρ (arcsec) (8)	λ (nm) (9)	$\Delta\lambda$ (nm) (10)
HR 1465	B 2092AB	29305	21281	04340—5503	99.7681	...	<0.22	541	88
...	99.7706	...	<0.22	541	88
...	99.7736	...	<0.22	541	88
...	99.7844	...	<0.26	644	128
HR 1481	KUI 18	29503	21594	04382—1418	99.7655	352.6	1.03	541	88
...	99.7655	352.5	1.02	644	128
...	99.7681	352.6	1.04	541	88
...	99.7681	352.1	1.02	644	128
...	99.7736	353.5	1.02	541	88
...	99.7737	352.3	1.01	644	128
...	99.7763	351.0	1.03	541	88
...	99.7763	351.9	1.01	644	128
...	99.7789	353.4	1.06	541	88
...	99.7790	350.8	1.02	644	128
...	99.7817	353.1	1.02	541	88
HR 1504	HJ 3683AB	30003	21756	04403—5857	99.7790	90.0	3.47	541	88
...	99.7844	90.1	3.44	644	128
...	99.7845	90.3	3.44	541	88
ADS 3380	STN 9	29755	21763	04404—1940	99.7817	...	<0.22	541	88
BD—01 702	HDS 606	29870	21894	04424—0056	99.7818	247.2	0.46	541	88
ADS 3483	BU 552AB	30869	22607	04518+1339	99.7737	221.4	0.52	541	88
...	99.7737	225.3	0.51	644	128
...	99.7763	221.9	0.49	541	88 ^a
...	99.7763	226.4	0.50	644	128
...	99.7790	229.3	0.48	541	88 ^a
...	99.7790	223.9	0.54	644	128
...	99.7818	224.2	0.51	541	88
...	99.7818	224.8	0.52	644	128
ADS 3588	BU 314AB	31925	23166	04590—1623	99.7763	325.5	0.81	541	88
...	99.7818	325.5	0.82	541	88
ADS 3596	STT 93	32022	23277	05005+0506	99.7790	65.8	1.45	541	88 ^c
CD—35 2090	HDS 658	32846	23596	05044—3542	99.7737	188.1	0.91	541	88
...	99.7845	185.8	0.85	644	128
HR 1652	JC 9	32831	23595	05044—3529	99.7656	306.0	3.12	541	88
...	99.7791	306.2	3.20	541	88
HR 1695	33684	23840	05076—6324	99.7873	...	<0.26	644	128
ADS 3711	STT 98	33054	23879	05079+0830	99.7737	322.0	0.76	541	88
...	99.7738	321.6	0.75	644	128
...	99.7763	322.0	0.76	541	88
...	99.7763	321.4	0.75	644	128
...	99.7791	322.7	0.77	541	88
...	99.7791	322.0	0.77	644	128
...	99.7818	322.3	0.76	541	88
...	99.7819	321.9	0.76	644	128
...	99.7872	322.9	0.78	541	88
ADS 3728	A 2636	33236	23957	05089+0313	99.7845	172.6	0.38	541	88
ADS 3764	STF 652	33646	24203	05118+0102	99.7872	181.3	1.72	541	88
ADS 3799	STT 517AB	33883—4	24349	05135+0158	99.7845	238.2	0.62	541	88
ADS 3954	HJ 3752AB	35163	25045	05218—2446	99.7791	92.7	3.49	541	88
BD+02 934	A 2641	35112	25119	05226+0236	99.7846	236.0	0.99	541	88 ^a
CP—68 375	I 276	36584	25482	05270—6837	99.7792	162.5	1.38	541	88
ADS 4115	STF 728	36267	25813	05308+0557	99.7738	46.8	1.17	644	128
...	99.7845	47.1	1.16	541	88
ADS 4123	STF 729AB	36351	25861	05312+0318	99.7872	27.7	1.91	541	88
ADS 4134	HEI 42Aa	36486	25930	05320—0018	99.7818	320.4	0.32	541	88 ^c
ADS 4241	BU 1032AB	37468	26549	05387—0236	99.7846	286.5	0.24	541	88 ^c
ADS 4390	STF 795	38710	27386	05480+0627	99.7872	217.0	1.15	541	88
CD—48 1991	I 63AB	39177	27408	05482—4855	99.7792	16.5	1.03	541	88
BD+09 978	HEI 670	39007	27549	05500+0952	99.7764	267.6	0.98	541	88
ADS 4562	STT 124	40369	28302	05589+1248	99.7764	296.5	0.58	541	88
ADS 4617	A 2715AB	40932	28614	06024+0939	99.7764	...	<0.22	541	88
...	99.7820	...	<0.22	541	88
HR 2162	DUN 23AB	41824	28796	06048—4828	99.7764	120.1	2.62	541	88
...	99.7792	120.0	2.64	541	88
...	99.7846	119.8	2.63	541	88
CD—48 2308	I 156	45572	30591	06257—4811	99.7819	125.2	1.04	541	88

TABLE 2—Continued

HR, ADS, DM, etc. (1)	Discoverer Designation (2)	HD (3)	HIP (4)	WDS (α, δ J2000.0) (5)	Date (1900 +) (6)	θ (deg) (7)	ρ (arcsec) (8)	λ (nm) (9)	$\Delta\lambda$ (nm) (10)
HR 2364	BU 753AB	45871	30840	06287—3222	99.7846	42.9	1.20	541	88
CD—50 2241	R 65AB	46273	30953	06298—5014	99.7819	87.2	0.75	541	88 ^c
...	99.7873	86.7	0.75	644	128 ^c
CD—36 3009	BU 755AB	47144	31457	06354—3647	99.7846	259.7	1.52	541	88
CD—36 3031	RST 4819	47500	31637	06372—3659	99.7819	2.0	0.55	541	88
...	99.7847	4.2	0.53	541	88
HR 2468	I 5AB	48189	31711	06380—6132	99.7874	255.1	0.29	644	128 ^a
ADS 5487	AC 4	49662	32677	06490—1509	99.7874	333.6	0.52	541	88
BD—13 1741	STF 997AB	51250	33345	06561—1403	99.7874	343.0	2.84	541	88
HR 2937	FIN 324AB-C	61330	37096	07374—3458	99.7819	15.1	0.37	541	88
HR 2937	FIN 324AB	61330	37096	07374—3458	99.7819	...	<0.22	541	88
HR 3485	I 10Aa-B	74956	42913	08447—5442	99.7820	344.2	1.06	541	88
HR 6750	HJ 5014	165189-0	88726	18068—4325	99.7863	8.4	1.72	541	88
ADS 11950	HDO 150AB	176687	93506	19026—2953	99.7864	228.2	0.31	541	88 ^a
ADS 11989	H 126	177166	93661	19043—2132	99.7754	8.2	1.20	541	88 ^c
CD—37 13048	HJ 5084	177474	93825	19064—3704	99.7699	61.8	1.28	541	88 ^a
...	99.7781	62.1	1.28	541	88 ^a
HR 7278	GLE 3	179366	94789	19172—6640	99.7754	328.6	0.51	541	88
CP—59 7534	I 121	186957	97646	19507—5912	99.7836	151.4	0.79	541	88
ADS 13104	STF 2597	188405	98038	19553—0644	99.7672	103.5	0.44	541	88 ^a
...	99.7755	102.2	0.45	541	88 ^a
HR 7637	HO 276	189340	98416	19598—0957	99.7672	290.4	0.26	541	88 ^b
CD—38 13809	HDO 294	189386	98556	20012—3835	99.7782	25.6	1.15	541	88
HR 7625	189124	98608	20017—5923	99.7809	...	<0.22	541	88
HR 7808	R 321	194433	100852	20269—3724	99.7755	133.7	1.48	541	88
...	99.7783	133.2	1.47	541	88
...	99.7809	133.6	1.46	541	88
ADS 13887	SHJ 323AB	194943	101027	20289—1749	99.7672	195.1	1.26	541	88
...	99.7836	194.4	1.27	541	88
ADS 14073	BU 151AB	196524	101769	20375+1436	99.7673	340.5	0.50	541	88
...	99.7673	340.7	0.51	644	128
...	99.7726	338.3	0.51	541	88
...	99.7726	339.0	0.50	644	128
...	99.7755	341.6	0.48	644	128
...	99.7756	342.5	0.47	541	88
...	99.7783	339.5	0.51	644	128
...	99.7837	341.2	0.52	541	88
...	99.7837	340.9	0.50	644	128
...	99.7864	340.6	0.52	541	88
...	99.7864	339.9	0.50	644	128
ADS 14099	HU 200AB	196662	101923	20393—1457	99.7673	116.4	0.35	541	88 ^a
...	99.7809	115.8	0.34	541	88 ^a
HR 7900	196777	101984	20400—1808	99.7837	...	<0.22	541	88
BD—22 5522	HDS 2957	197711	102486	20462—2145	99.7837	114.5	0.89	541	88
ADS 14360	STF 2729AB	198571	102945	20514—0538	99.7673	20.1	0.94	541	88
ADS 14380	HJ 3003AB	198732	103071	20530—2347	99.7810	198.2	1.64	541	88
ADS 14430	STF 2735	199223	103301	20557+0432	99.7837	282.1	2.07	541	88
ADS 14499	STF2737AB	199766	103569	20591+0418	99.7726	285.3	0.81	541	88
...	99.7837	286.1	0.81	541	88
ADS 14573	STF 2744AB	200375	103892	21031+0132	99.7727	118.5	1.33	541	88
ADS 14592	STF 2745Aa-B	200497	103981	21041—0549	99.7837	197.1	2.47	541	88
ADS 14666	STT 527	201221	104324	21080+0509	99.7810	299.3	0.31	541	88 ^b
CD—41 14503	BU 766AB	203585	105696	21244—4100	99.7811	210.0	0.26	541	88 ^a
CD—43 14539	MLO 6	204018	105913	21270—4233	99.7811	150.1	2.89	541	88
ADS 15007	STF 2799AB	204509	106053	21289+1105	99.7838	264.0	1.82	541	88
ADS 15176	BU 1212AB	206058	106942	21395—0003	99.7810	273.5	0.54	541	88
CP—83 722	HJ 5278	206240	107843	21509—8243	99.7811	62.4	3.31	541	88
...	99.7865	62.4	3.30	644	128
CD—29 18119	BU 276	209014	108661	22008—2827	99.7812	113.4	1.84	541	88
...	99.7866	113.3	1.83	644	128
HR 8462	HDS 3152	210705	109624	22124—1412	99.7812	267.3	0.58	541	88
ADS 15902	BU 172AB	212404	110578	22241—0450	99.7812	246.6	0.28	541	88 ^b
...	99.7866	64.2	0.29	644	128 ^a
ADS 15934	SHJ 345AB	212697-8	110778	22266—1645	99.7812	5.7	1.74	541	88
...	99.7867	5.5	1.74	644	128
ADS 15971	STF 2909AB	213051-2	110960	22288—0001	99.7591	187.8	1.98	541	88

TABLE 2—Continued

HR, ADS, DM, etc. (1)	Discoverer Designation (2)	HD (3)	HIP (4)	WDS (α, δ J2000.0) (5)	Date (1900+) (6)	θ (deg) (7)	ρ (arcsec) (8)	λ (nm) (9)	$\Delta\lambda$ (nm) (10)
...	99.7648	188.0	1.95	541	88
...	99.7648	187.9	1.94	644	128
...	99.7728	188.1	1.95	541	88
...	99.7756	187.9	1.95	541	88
ADS 15988	STF 2912	213235	111062	22300+0426	99.7729	119.6	0.40	541	88 ^a
...	99.7757	118.1	0.40	541	88
...	99.7757	293.9	0.36	644	128 ^b
...	99.7811	119.3	0.39	541	88 ^a
...	99.7838	117.7	0.38	541	88 ^a
HR 8582	213442	111310	22330-6159	99.7760	...	<0.22	541	88
HR 8629	KUI 114	214810	111965	22408-0333	99.7757	...	<0.26	644	128
...	99.7867	...	<0.26	644	128
...	99.7948	...	<0.22	541	88
ADS 16173	HO 296AB	214850	111974	22409+1433	99.7674	31.1	0.33	541	88 ^a
...	99.7674	28.8	0.33	644	128 ^a
HR 8636	214952	112122	22427-4653	99.7729	...	<0.22	541	88
CP-63 4826	I 340	216187	112924	22522-6311	99.7838	336.1	0.87	541	88
...	99.7949	336.8	0.87	541	88
ADS 16365	BU 178	216718	113184	22552-0459	99.7702	319.2	0.66	541	88
...	99.7757	321.6	0.69	644	128
...	99.7867	321.9	0.69	644	128
...	99.7948	322.3	0.69	541	88
...	99.7948	320.7	0.70	644	128
CD-46 14497	HU 1335	217084	113454	22586-4531	99.7649	106.9	0.41	644	128 ^a
CD-37 15047	BU 1011	217642	113784	23026-3625	99.7839	293.5	2.04	541	88
...	99.7949	292.9	2.08	541	88
HR 8787	JC 20AB	218227	114131	23069-4331	99.7729	106.9	1.42	541	88
...	99.7757	107.1	1.41	644	128
CD-39 14936	BU 773	218242	114132	23069-3854	99.7839	206.2	0.98	541	88
...	99.7949	208.7	0.97	541	88
ADS 16649	BU 79AB	219657	115012	23176-0131	99.7757	14.4	1.62	644	128
...	99.7949	16.2	1.56	541	88
HR 8877	RST 5560AB	220003	115272	23208-5018	99.7839	234.5	1.28	541	88
...	99.7949	232.5	1.32	541	88
ADS 16708	HU 295	220278	115404	23227-1502	99.7867	262.4	0.26	644	128 ^a
CP-67 3964	HDS 3340	220759	115756	23271-6635	99.7838	206.1	0.25	541	88 ^b
CD-28 18220	HDS 3343	221083	115916	23291-2816	99.7675	316.3	0.57	541	88
BD-21 6437	B 1900	221565	116247	23333-2055	99.7729	124.8	0.74	541	88
...	99.7758	124.7	0.76	541	88
CD-28 18257	SEE 492	221839	116436	23357-2729	99.7648	352.1	0.56	541	88
...	99.7648	350.3	0.56	644	128

^a Quadrant ambiguous, but consistent with previous measures in the CHARA Third Catalog.

^b Quadrant ambiguous, but inconsistent with previous measures in the CHARA Third Catalog.

^c Quadrant unambiguous, but inconsistent with previous measures in the CHARA Third Catalog.

Table 4 and, therefore, were not used to determine the measurement precision. Filled circles indicate the measures used to calculate the values in Table 4. All points are plotted with error bars; these are the ephemeris uncertainties as determined from the published orbit. The plots and Table 4 both indicate no significant discrepancies and no systematic trends between the astrometric determinations here and the predicted positions. Because of the quality of the orbits used in the study, we may roughly associate the scatter in the residuals with the measurement precision limitations. The figure for separation measurement error in Table 4 is slightly lower than that obtained by Douglass et al. (1999) on a comparably sized telescope but comparable with an earlier paper in that series (Germain, Douglass, & Worley 1999). The separation measurement error is also larger than in Paper I, but this may be attributed to at least in part to the much better seeing conditions (1".2 to 1".3) of the earlier run.

The separations used in the speckle orbit study are mostly below 1" and do not span the range of measures presented in Table 2. It is, therefore, possible that pixel scale determination could be systematically off at a level that would not be detected in small separation objects but would be evident at larger separations. To investigate this possibility, we completed a second residual study based on a small group of wide ($\rho > 2''.0$), very slow moving pairs, comparing our measures with the last measure appearing in the CHARA Third Catalog of Interferometric Measurements of Binary Stars (Hartkopf, McAlister, & Mason 1997). In this case, we were primarily interested in looking for a systematic offset in position angle or separation, and not in the rms deviation of the residuals. Figures 3a and 3b show the results of 10 such measures. There appears to be no offset in either parameter even in these larger separation systems: the average residual in position angle was $\overline{\Delta\theta} = 0''.02$

TABLE 3
POSITION ANGLE AND SEPARATION CHANGES SINCE THE *Hipparcos* OBSERVATION EPOCH FOR *Hipparcos* DISCOVERY OBJECTS

Discoverer Designation (1)	HIP (2)	Total <i>V</i> Magnitude (3)	Magnitude Difference (4)	π (mas) (5)	HIP θ (deg) (6)	HIP ρ (arcsec) (7)	$\Delta\theta$ (deg) (8)	$\Delta\rho$ (arcsec) (9)
HDS 95	3385	7.22	2.83	8.41	341	0.874	-3	-0.03
HDS 107	3804	7.95	3.15	7.46	294	0.645	+8	+0.21
HDS 154	5514	7.98	2.32	10.91	284	0.735	+5	-0.06
HDS 325	11644	6.50	2.46	9.39	78	0.518	-4	+0.06
.....	+2	+0.05
.....	0	+0.04
.....	-3	+0.04
.....	+6	+0.07
.....	-8	+0.10
HDS 505	18731	7.03	0.58	6.56	265	0.308	+1	+0.01
.....	-6	+0.00
HDS 606	21894	6.73	2.25	7.06	247	0.468	0	+0.01
HDS 658	23596	6.32	3.11	9.77	183	0.886	+5	+0.02
HDS 2957	102486	7.82	3.12	30.10	91	1.105	+24	-0.21
HDS 3152	109624	6.04	3.15	23.00	257	0.602	+10	-0.02
HDS 3340	115756	6.47	1.98	3.68	27	0.300	-4	-0.05
HDS 3343	115916	7.66	2.13	4.48	318	0.566	-2	0.00

$\pm 0^{\circ}.21$ degrees, and for the separation the result was $\overline{\Delta\rho} = 3.3 \pm 10.1$ mas. However, the number of measures of this type is small, and it is not possible to completely rule out small systematic errors from the scale and zero-point angle determinations.

As a final test of the measurement precision, we examined the objects in Table 2 that have five or more measures. The random errors in position angle and separation were estimated by computing the standard deviation of the values

obtained. The position angle deviations are shown in Figure 4a as a function of the average separation value for the objects. These exhibit a trend toward higher values at smaller separations, as expected for a constant linear measurement error. Plotted with the data points is a curve representing the function $\sigma_{\theta} = 0.75/\rho$, which would be the curve expected for a rectilinear measurement precision uncertainty of 13.1 mas (i.e., equal to that of the separation residuals obtained earlier). The curve agrees with the data

TABLE 4
SUMMARY OF RESIDUALS, SPECKLE ORBITS

Orbit Requirement	Number of Measures	Average Residual (obs-eph)	RMS Dev. from Ave. Res.
$\delta\theta_{\text{eph}} < 1^{\circ}.0$	19	$\overline{\Delta\theta} = -0^{\circ}.33 \pm 0^{\circ}.42$	$\sigma_{\theta} = 1^{\circ}.76 \pm 0^{\circ}.29$
$\delta\rho_{\text{eph}} < 6.5$ mas	20	$\overline{\Delta\rho} = -2.8 \pm 3.0$ mas	$\sigma_{\rho} = 13.1 \pm 2.1$ mas

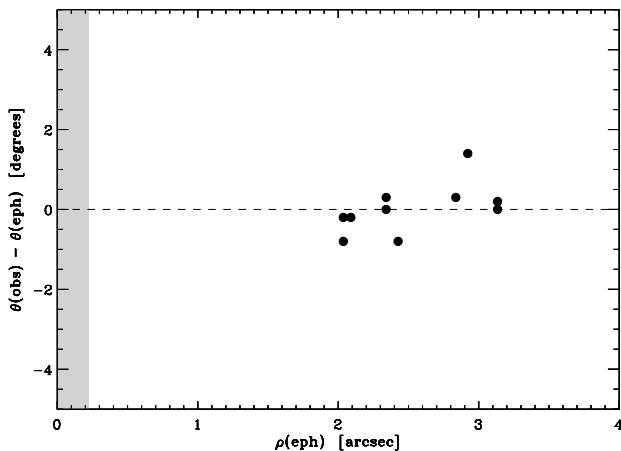


Fig.3a

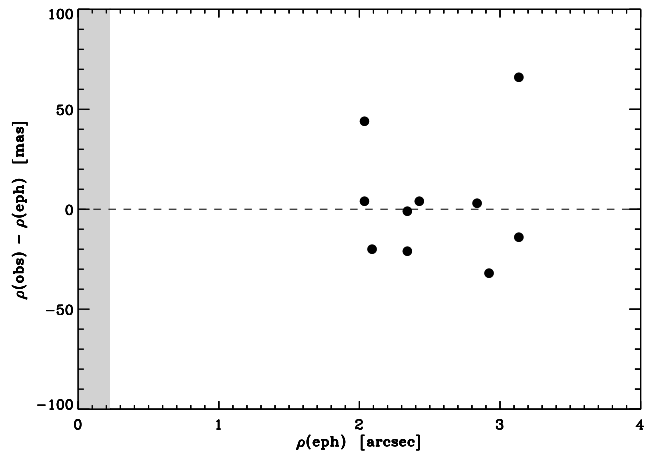


Fig.3b

FIG. 3.—(a) Position angle residuals plotted as a function of the last observed separation appearing in the CHARA Third Catalog for objects in Table 2 that have appeared nearly stationary over a long history of observations. (b) Separation residuals plotted as a function of the last observed separation appearing in the CHARA Third Catalog for the same set of observations. The gray band in both plots marks the region below the diffraction limit of the telescope (at *V*).

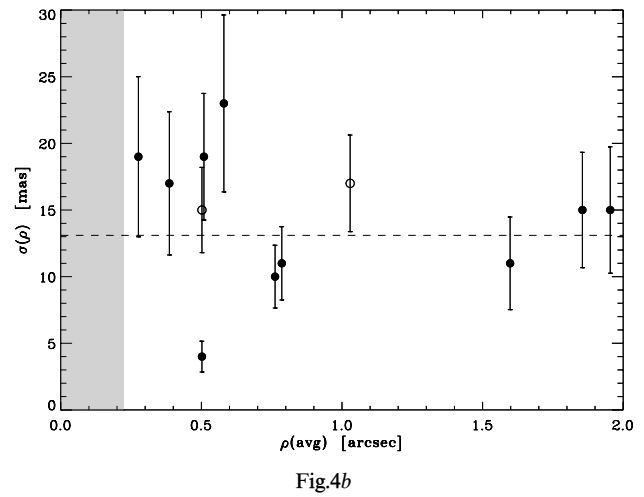
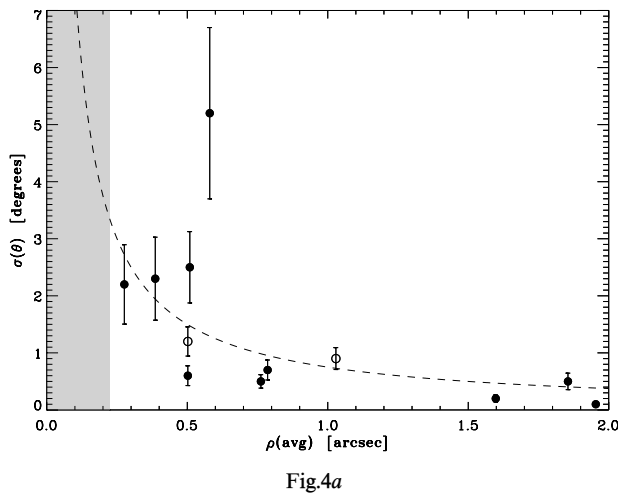


FIG. 4.—(a) Position angle standard deviations plotted as a function of average separation from Table 2 for objects observed five or more times. The dotted line is the function $\sigma_\theta = 0.75/\rho$, where the units of σ are degrees and for ρ are arcseconds. (b) Separation standard deviations for the same objects. The dotted line marks the rms deviation obtained from the speckle orbit study. In both plots, the open circles indicate BU 151AB and KUI 18, two objects that were also used in the speckle orbit study. The gray band marks the region below the diffraction limit of the telescope (at V).

reasonably well. Figure 4b shows the separation deviations as a function of average separation obtained on each object; these appear to be consistent with the 13.1 mas figure for the measurement precision also and show no systematic trend as a function of separation. Figure 5 shows the separation deviations plotted as a function of (Fig. 5a) the total V magnitude of the objects and (Fig. 5b) the magnitude difference of the objects. Both the magnitudes and magnitude differences used were drawn from the *Hipparcos* Catalogue. Independent magnitude differences were derived for all objects in the course of our analysis; these will be the subject of a forthcoming paper. Error bars plotted for the magnitude differences in Figure 5b are 0.14 mag; this figure was obtained by Mignard et al. (1995) for *Hipparcos* data. The former plot shows no significant trend with total magnitude, but the measurement precision does appear to decrease (meaning that the standard deviation increases) for large magnitude difference systems. Overall, the results of

this study are fully consistent with those of the first study involving the speckle orbits, indicating measurement precision of about 13 mas in separation and $0.75/\rho$ degrees, where ρ is the separation of the system measured in arcseconds.

Figure 6 shows a plot of magnitude difference versus total magnitude for all of the systems observed during our run; it appears similar to that presented in Paper I. Although it is difficult to judge the true magnitude difference detection limit, Figure 6 suggests that systems brighter than 8th magnitude and with magnitude differences less than 3 to 4 can generally be successfully measured with this telescope/instrument combination. There is also an indication that the sensitivity to large magnitude differences decreases as the total magnitude becomes fainter; this is expected from power spectrum signal-to-noise considerations.

The reduction scheme occasionally returns the quadrant that is inconsistent with previous measures reported by

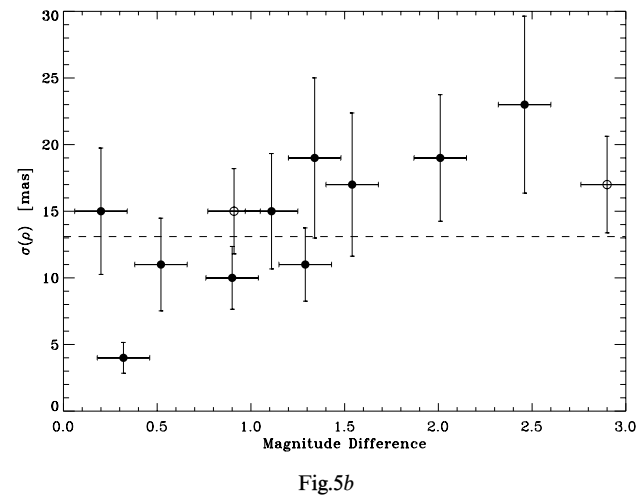
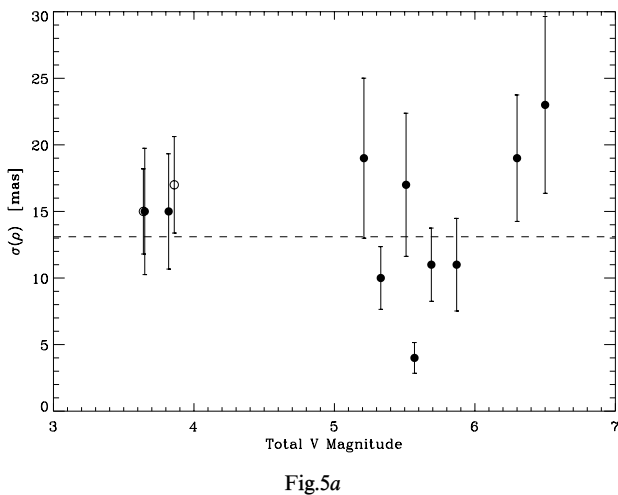


FIG. 5.—(a) Separation standard deviations plotted as a function of total magnitude for the objects in Table 2 observed 5 or more times. (b) Separation standard deviations plotted as a function of magnitude difference (as given in the *Hipparcos* Catalogue) for the same objects. The dotted line here marks the rms deviation obtained from the speckle orbit study. In both plots, the open circles indicate BU 151AB and KUI 18, two objects that were also used in the speckle orbit study.

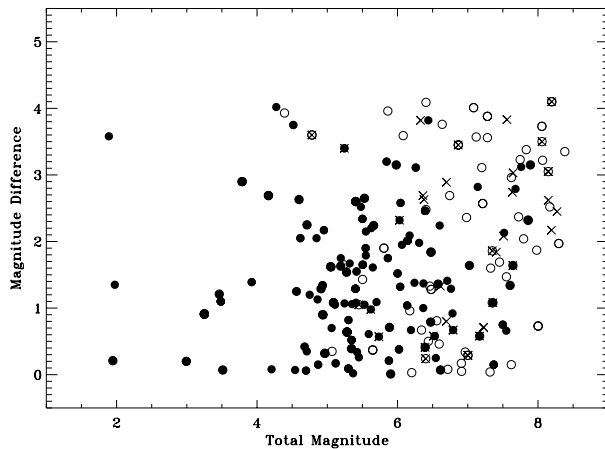


FIG. 6.—Magnitude difference plotted as a function of total V magnitude for all systems observed during the run, except nondetections of systems presumed to be below the diffraction limit based on orbital data. Values of both coordinates are taken from the *Hipparcos* Catalogue. Filled circles are successfully analyzed systems for which measures appear in Table 2, open circles are systems where the secondary was detected but the observation failed one or more criteria for high-quality astrometry, and crosses are systems where the secondary was not detected. Error bars in the magnitude differences are omitted for clarity.

other observers (i.e., our position angle is off by 180° relative to previous determinations; such cases are noted in Table 2). These are usually small magnitude difference systems, but large magnitude difference systems can also be affected.

These larger Δm systems tend to have small separations, indicating that quadrant determinations made with our measurement technique may be less reliable near the diffraction limit. We will continue to investigate this possibility with future observations.

4. CONCLUSIONS

We have presented 280 position angle and separation measures, as well as 23 nondetections, of double stars derived from speckle interferometry data taken at the Lowell-Tololo Telescope in October of 1999. These data are characterized by rms deviations of 1.8 ± 0.3 in position angle and 13 ± 2 mas in separation. Despite significantly poorer seeing than the data presented in Paper I, the detection capabilities appear similar, with systems of total magnitude brighter than 8 and magnitude difference less than 4 being measurable.

We are grateful to R. Millis of Lowell Observatory for his support of this project; C. Enterline, O. Saa, and D. Maturana of CTIO for their help before and during the observing run; R. Argyle of the Institute for Astronomy, Cambridge, UK, for advice on the target list; R. Easton of RIT for a timely loan of equipment; and the referee for comments regarding a few objects in Table 2. This work was funded by a grant from NASA administered by the American Astronomical Society and JPL subcontract 1201846 from the Preparatory Science Program for the Space Interferometry Mission.

REFERENCES

- Argue, A. N., Hebden, J. C., Morgan, B. L., & Vine, H. A. 1984, *MNRAS*, 206, 669
- Bessel, M. S. 1990, *PASP*, 102, 1181
- Douglass, G. G., Mason, B. D., Germain, M. E., & Worley, C. E. 1999, *AJ*, 118, 1395
- ESA. 1997, *The Hipparcos and Tycho Catalogue* (ESA SP-1200) (Noordwijk: ESA)
- Germain, M. E., Douglass, G. G., & Worley, C. E. 1999, *AJ*, 117, 1905
- Gunn, J. E., & Stryker, L. L. 1983, *ApJS*, 52, 121
- Hartkopf, W. I., Mason, B. D., Barry, D. J., McAlister, H. A., Bagnuolo, W. G., & Prieto, C. M. 1993, *AJ*, 106, 352
- Hartkopf, W. I., Mason, B. D., & McAlister, H. A. 1996, *AJ*, 111, 370
- Hartkopf, W. I., Mason, B. D., McAlister, H. A., Turner, N. H., Barry, D. J., Franz, O. G., & Prieto, C. M. 1996, *AJ*, 111, 936
- Hartkopf, W. I., McAlister, H. A., & Franz, O. G. 1989, *AJ*, 98, 1014
- Hartkopf, W. I., McAlister, H. A., & Mason, B. D. 1997, *Third Catalog of Interferometric Measurements of Binary Stars* (CHARA Contrib. No. 4) (Atlanta: Georgia State Univ.)
- Hoffleit, D., & Jaschek, C. 1982, *The Bright Star Catalogue* (4th ed.; New Haven: Yale Univ. Obs.)
- Horch, E. P., Dinescu, D. I., Girard, T. M., van Altena, W. F., López, C. E., & Franz, O. G. 1996, *AJ*, 111, 1681
- Horch, E. P., Girard, T. M., van Altena, W. F., Meyer, R. D., López, C. E., & Franz, O. G. 1997, in *Visual Double Stars: Formation, Dynamics and Evolutionary Tracks*, ed. J. A. Döbbo, A. Elipse, & H. McAlister (Dordrecht: Kluwer), 43
- Horch, E. P., Ninkov, Z., & Slawson, R. W. 1997, *AJ*, 114, 2117 (Paper I)
- Jacoby, G. H., Hunter, D. A., & Christian, C. A. 1984, *ApJS*, 56, 257
- Kavaldjiev, D., & Ninkov, Z. 1998, *Opt. Eng.*, 37, 948
- Mason, B. D. 1997, *AJ*, 114, 808
- Mason, B. D., Douglass, G. G., & Hartkopf, W. I. 1999, *AJ*, 117, 1023
- McAlister, H. A., Hartkopf, W. I., & Franz, O. G. 1990, *AJ*, 99, 965
- Mignard, F., et al. 1995, *A&A*, 304, 94
- Morgan, B. L., Beckmann, G. K., & Scaddan, R. J. 1980, *MNRAS*, 192, 143
- Morgan, B. L., Beckmann, G. K., Scaddan, R. J., & Vine, H. A. 1982, *MNRAS*, 198, 817
- Morgan, B. L., Beddoes, D. R., Scaddan, R. J., & Dainty, J. C. 1978, *MNRAS*, 183, 701
- van Altena, W. F., Lee, J. T., Lee, J.-F., Lu, P. K., & Upgren, A. R. 1988, *AJ*, 95, 1744
- White, G. L., Jauncey, D. L., Reynolds, J. E., Blackmore, D. R., Matcher, S. J., Morgan, B. L., Vine, H. A., & Argue, A. N. 1991, *MNRAS*, 248, 411
- Worley, C. E., & Douglass, G. G. 1997, *A&AS*, 125, 523
- Worley, C. E., & Heintz, W. D. 1983, *Fourth Catalog of Orbits of Visual Binary Stars* (Publ. US Nav. Obs., 2d Ser., 24, Part 7) (Washington: GPO)